Research Article

New Insight Into the Evaluation of Abnormal Left Ventricular Wall Motion

Yoichi Nakamura[*]

Specified Clinic of Soyokaze CardioVascular Medicine and Diabetes Care, Division of Cardiovascular Medicine, Matsuyama, Japan

*Corresponding Author: Yoichi Nakamura, Specified Clinic of Soyokaze CardioVascular Medicine and Diabetes Care, Division of Cardiovascular Medicine 73-1 Muromachi, Matsuyama, Ehime, 790-0026, Japan

Citation: Yoichi Nakamura. New Insight Into the Evaluation of Abnormal Left Ventricular Wall Motion. Cardiology and Cardiovascular Medicine 4 (2021): 404-416.

Abstract

Background: Previous predictors of mechanical dyssynchrony using echocardiography has not improved refractory heart failure in patients treated with cardiac resynchronization therapy. It was hypothesized that the spatially and temporary continuous information of the whole endocardium is required when the mechanical dyssynchrony is assessed using echocardiography. This study aimed to examine differences in the locus of the centroid of the left ventricle between wall motion abnormality.

Methods: Twenty-seven patients with dilated cardiomyopathy and 45 old myocardial infarction patients with aneurysm were compared with 188 individuals with normal wall motions. In an off-line system, the centroid of the three-dimensional left ventricle was defined as the central point between both centroids calculated from four- and two-chamber images using an original application.

Results: The locus of the centroid of the left ventricle (LCGLV) in the normal group showed a horizontally inverted β shape, whereas this shape was absent in the other groups. When corrected by left ventricular end-systolic volume, the total and each directional length of LCGLV in the abnormal wall motion groups were clearly reduced compared with those recorded in the normal group. The acceleration of the centroid was also reduced in the abnormal wall motion groups. Multiple linear regression analysis with a stepwise method revealed a corrected antero-posterior shift of the centroid of left ventricle by left ventricular end-systolic volume and N-terminal pro-brain natriuretic peptide, which strongly correlated with the LVEF (adjusted R^2: 0.6818, $p \leq 2.2 \times 10^{-16}$).

Conclusion: Use of the LCGLV provides novel insight into the evaluation of abnormal left ventricular contractions.

Trial registration: Retrospectively registered

Abbreviations

DCM, dilated cardiomyopathy

EchoCRT, echocardiography guided cardiac resynchronization therapy

LV, left ventricle

LVEF, left ventricular ejection fraction

LVESV, left ventricular end-systolic volume

NWM, normal wall motion

OMI, old myocardial infarction

PROSPECT, predictors of response to cardiac resynchronization therapy

1. Background

In the last century, echocardiography emerged in the clinical field as a visualization tool for the evaluation of cardiac anatomical and pathological abnormalities, as well as the flow dynamics of heart diseases [1]. With the technological development, this diagnostic tool has contributed to the evaluation of cardiac diseases, such as cardiomyopathies, ischemic heart diseases, valvular heart diseases, etc. However, despite the development of several techniques, the objective judgement of the left ventricular (LV) wall motion remains a challenge. For example, it is recognized that cardiac resynchronization therapy is a therapeutic strategy for patients with medical resistant refractory heart failure in whom LV systolic function is severely reduced. The European Society of Cardiology guidelines established in 2016 and 2019 stated that patients with a symptomatic sinus rhythm, reduced LV ejection fraction (LVEF), prolonged conduction time which met the QRS duration ≥130 ms, and a left bundle branch block shape on an electrocardiogram could be responders to cardiac resynchronization therapy [2,3]. As demonstrated in the PROSPECT study [4] and ECHO-CRT trial [5], echocardiography is unable to

identify responders to this novel therapeutic strategy. Previous echocardiographic assessment of mechanical dyssynchrony was limited to regional LV wall information utilizing a tissue Doppler technique or M-mode evaluation, although the heart is a three-dimensional moving muscle. Blood flow was also assessed using a pulse Doppler technique, which estimated the LV dysfunction using the time difference obtained from the blood stream at the LV and right ventricle inflow/outflow. Obviously, this was indirect information and did not critically reflect the whole LV wall motion. Therefore, the present author presumed that the accurate evaluation of LV dyssynchrony requires information for each wall of the heart during a consecutive cardiac cycle, particularly to determine the suitability of resynchronization therapy. In the present study, it was hypothesized that the centroid of the LV reflects a cardiac wall motion because this technique requires the spatial coordinates of each endocardial position on the LV wall with time information during a cardiac cycle. Therefore, the locus of the centroid could include information on each regional area, such as the presence of interstitial/replacement fibrosis which limits LV contraction. This study investigated the role of the locus of the centroid in the assessment of abnormal LV wall motion as a novel approach differentiated from previous methods.

2. Methods

2.1 Study population

Continuous digital videos of 633 patients, obtained from the clinical echocardiography laboratory from September 2016 to August 2017, were utilized in this study. Cases of dilated cardiomyopathy (DCM) and old myocardial infarction (OMI) with aneurysm were evaluated. Cases of valvular heart disease, OMI without aneurysm, congenital structure cardiac disease, pulmonary hypertension, and those with images of poor quality were excluded from the study. The remaining videos that showed normal wall motion (NWM) of the LV were also used in this

study as control. The protocol of this retrospective study was approved by the SOYOKAZE CVD ethics committee (soyokaze-cvd, 2018-03). The purpose of this study was conveyed to the patients on the information board and the website homepage of the clinic. An opt-out option was provided to patients who did not wish to participate in the study.

2.2 Two-dimensional tissue tracking system of the LV

Audio/video interleave files, obtained during one cardiac cycle using a trans-thoracic echocardiography equipped with a high-resolution sector probe (AVIUS; Hitachi Ltd., Tokyo, Japan), were evaluated. The two-dimensional speckle tracking algorithm (Hitachi Ltd.) is a pattern-matching method which forwards dozens of pixels into the region of interest (1 cm^2) through an off-line system using an application termed '%WT' programmed in e-Tool viewer (Hitachi Ltd.) [6,7]. In this off-line system, approximately 50 points were automatically allocated on the manually traced line as the border of the endocardium. The coordinates of each point, which were followed frame by frame during one cardiac cycle, were saved as a comma-separated value file.

2.3 Locus of the centroid of the LV

The locus of the centroid of the LV was subsequently calculated through each frame image using an original application. The centroid of the three-dimensional LV was identified as the middle point between the centroid of the four-chamber image and that of the two-chamber image. The locus of the centroid of the three-dimensional LV was also shown on the same sheet. The volume calculated from the x-, y-, z-transfer distance which the centroid of the three-dimensional LV had moved toward each direction during one cardiac cycle was defined as the box volume, indicating a moving space of the LV centroid. To evaluate the relationship between a three-dimensional centroid and LV systolic function, any markers obtained from the locus of a three-

dimensional centroid (e.g., length, volume, acceleration) were compared with LVEF. Also, their relationship with any markers of LV diastolic function, QRS duration on electrocardiogram or the value of N-terminal pro-brain natriuretic peptide (NT-proBNP) was also assessed.

2.4 Statistical analysis

The data are shown as medians with the first and third quartile values because of a non-normal distribution of data. Qualitative data were assessed through Fisher's exact test. Non-parametric data for each group were processed by Kruskal–Wallis analysis with a post-hoc method. Univariate and multivariate linear regression analyses were applied to identify the independent predictors of the LVEF. The correlation between the markers of the LV centroid and the measured data of LV diastolic function was evaluated by Spearman's rank correlation coefficient. NT-proBNP and QRS duration on electrocardiography were also assessed using this correlation coefficient. A p-value <0.05 denoted a statistically significant association in the final model. All statistical analyses were performed with EZR (Saitama Medical Center, Jichi Medical University, Saitama, Japan), which is a graphical user interface for R (The R Foundation for Statistical Computing, Vienna, Austria). More precisely, it is a modified version of R commander designed to include additional statistical functions frequently used in biostatistics [8].

3. Results

A total of 260 patients were evaluated in this study. Patient background information is summarized in Table 1. The findings of physiological examination and a biomarker analysis for each group are summarized in Table 2. Representative images of the centroid of the LV in each group are demonstrated in figure 1.

	DCM group	OMI group	NWM group	p-value
N	27	45	188	
Age, years (median [quartile])	74 (64–79)	72 (66–82)	64 (52–74)	$1.47×10^{-5}$
Sex, Female/Male, N	Sep-18	Apr-41	103/85	$1.26×10^{-8}$
Medication				
β-blocker	22 (81%)	33 (73%)	54 (29%)	$1.03×10^{-11}$
ACE-I/ARB	12 (44%)	21 (47%)	77 (41%)	0.835
Calcium-antagonist	9 (33%)	13 (29%)	66 (35%)	0.77
Digitalis	2 (7%)	1 (2%)	0	0.011
Diuretics	9 (33%)	20 (44%)	4 (2%)	$1.03×10^{-14}$
Anti-aldosterone	9 (33%)	12 (27%)	7 (6%)	$5.21×10^{-8}$
α-blocker	4 (15%)	4 (9%)	35 (17%)	0.302
Nitrate	0	6 (13%)	3 (2%)	0.0035
Statin	17 (63%)	34 (76%)	89 (47%)	0.0016

ACE-I, angiotensin-converting enzyme inhibitor; ARB, angiotensin II receptor blocker; DCM, dilated cardiomyopathy; NWM, normal wall motion; OMI, old myocardial infarction

Table 1: Background information of patients in each group

	DCM group	OMI group	NWM group	p-value
Echocardiography				
LVDd (mm)	58 (55–62)	58 (51–65)	49 (45–51)	$1.38×10^{-18}$
LVDs (mm)	46 (40–48)	44 (36–51)	30 (26–33)	$5.67×10^{-24}$
LVEDV (ml)	118 (97–163)	136 (113–172)	89 (75–104)	$2.11×10^{-12}$
LVESV (ml)	70 (57–90)	83 (56–106)	34 (28–41)	$1.46×10^{-40}$
LVEF (%)	43 (39–47)	38 (30–43)	61 (58–64)	$1.34×10^{-30}$
E/A	0.74 (0.7–0.9)	0.73 (0.6–1.1)	0.95 (0.7–1.2)	0.0071
E/e'	7.2 (5.6–11.0)	9.1 (6.4–12.4)	6.5 (5.2–8.8)	$5.23×10^{-5}$
LA volume (ml)	67 (57–91)	57 (48–75)	44 (36–56)	$2.44×10^{-10}$
Electrocardiography				
AF/NSR	7/20	3/42	1/187	$1.12×10^{-6}$
QRS width (ms)	104 (93–123)	102 (90–114)	92 (86–98)	$3.21×10^{-6}$
Biomarker				
NT-proBNP (pg/ml)	923 (266–2390)	809 (280–1650)	82.5 (44–159)	$1.75×10^{-23}$

Data are presented as medians with first and third quartile values.

AF, atrial fibrillation; DCM, dilated cardiomyopathy; LVDd, left ventricular diameter of the diastole; LVDs, left ventricular diameter of the systole; LVEDV, left ventricular end-diastolic volume; LVEF; left ventricular ejection fraction; LVESV; left ventricular end-systolic volume; NSR; normal sinus rhythm; NT-proBNP, N-terminal pro-brain natriuretic peptide; NWM, normal wall motion; OMI, old myocardial infarction

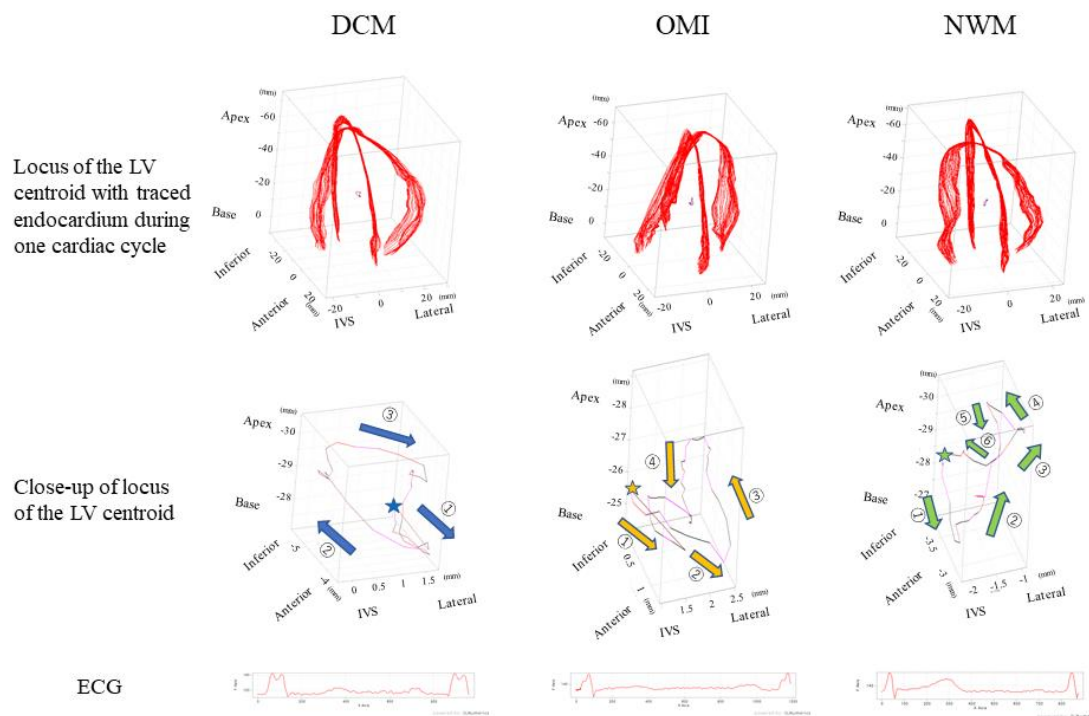**Table 2:** Physiological examination and biomarker data for each group

Figure 1: Representative images of the locus of the centroid of the left ventricle for each group. The top panels show the outline of the endocardium (red lines) obtained from an apical four-chamber view (x-axis) with a two-chamber view (y-axis) of the left ventricle drawn in the same cubic together with all frames of the endocardium lines accompanied by the locus of the centroid of the left ventricle. The middle panels indicate the close-up of the locus of the centroid of the left ventricle. The stars in each illustration indicate a starting point on a systolic period, which revealed the starting point of the QRS spike on the electrocardiogram. Normal left ventricular wall motion showed that the centroid of the left ventricle shifted to the frontal portion during an early systolic phase (green arrow 1); thereafter, that point rapidly moved toward the apical site (green arrows 2 and 3). Subsequently, it returned to the starting point with two loose loops during a diastolic phase and an atrial contraction (green arrows 4–6), resembling a mirror image of a β shape. The DCM group showed movement in a swinging motion on the box like a load with clockwise rotation (blue arrows). The OMI group showed that the locus formed a crashed inverted β shape with counterclockwise rotation (brown arrows). The bottom panels show the electrocardiogram of each group. DCM, dilated cardiomyopathy; ECG, electrocardiogram; IVS, interventricular septum; LV, left ventricle; NWM, normal wall motion; OMI, old myocardial infarction.

Firstly, the locus of the centroid that belonged to the NWM group had rapidly moved toward the anterior portion during the early systolic phase; thereafter, it shifted toward the apical direction. Subsequently, it returned to the original position through a diastolic relaxation phase and an atrial contraction stage; during this phase, the centroid moved in the counterclockwise direction on the same sheet frame by frame. Consequently, the locus of the centroid of the NWM group showed a horizontal inverted β shape. The representative image of the DCM group demonstrated in figure 1 shows a box-like shape of the centroid of the three-dimensional LV and clockwise directional rotation. The representative

locus image of the OMI group showed a crashed inverted β shape. The actual locus length and the box volume of the centroid were not significantly different among the groups (Figures 2a, 2b). However, when corrected by the LV end-systolic volume (LVESV), the length of the locus of the centroid of the DCM group (median value: 0.168 mm^{-2} [0.150–0.195 mm^{-2}]) and OMI group (mean value: 0.159 mm^{-2} [0.120–0.220 mm^{-2}]) was significantly shorter than that of the NWM group (median value: 0.379 mm^{-2} [0.305–0.493 mm^{-2}]; $p=7.85\times10^{-26}$) (Figure 2c). The corrected box volume of the abnormal wall motion groups (median value, DCM group: 0.007 [0.004–0.010]; OMI group: 0.008 [0.004–0.006]) was also smaller than that calculated in the NWM group (median value: 0.011 [0.007–0.015]; $p=1.20\times10^{-8}$) when corrected by LVESV (figure 2d). In the DCM group, the locus length of the centroid for the lateral and antero-posterior directions was longer than that of the NWM group (figures 3a, 3b); nevertheless, the length for the longitudinal direction was shorter than that of the NWM group (figure 3c). When these data were

corrected by LVESV, the lengths were significantly reduced compared with those obtained from the NWM group (figures 3d, 3e). The corrected longitudinal length of the abnormal wall motion groups was markedly reduced compared with that of the NWM group (figure 3f). The maximum acceleration of the LV centroid obtained for the DCM group (median value: 698 mm/s^2 [547–775 mm/s^2]) and OMI group (median value: 724 mm/s^2 [565–965 mm/s^2]) were reduced compared with that of the NWM group (median value: 878 mm/s^2 [713–1,112 mm/s^2]; $p=7.49\times10^{-7}$) (figure 4a). On the other hand, the minimum acceleration of the LV centroid of the abnormal wall motion groups (median value, DCM group: −624 mm/s^2 [−522−−776 mm/s^2]; OMI group: −589 mm/s^2 [−507–804 mm/s^2]) was higher than that of the NWM group (median value: −826 mm/s^2 [−668−−974 mm/s^2]; $p=4.12\times10^{-7}$) (Fig. 4b). When the acceleration values were corrected by LVESV, those of the abnormal wall motion groups were lower compared with those of the NWM group (figures 4c, 4d).
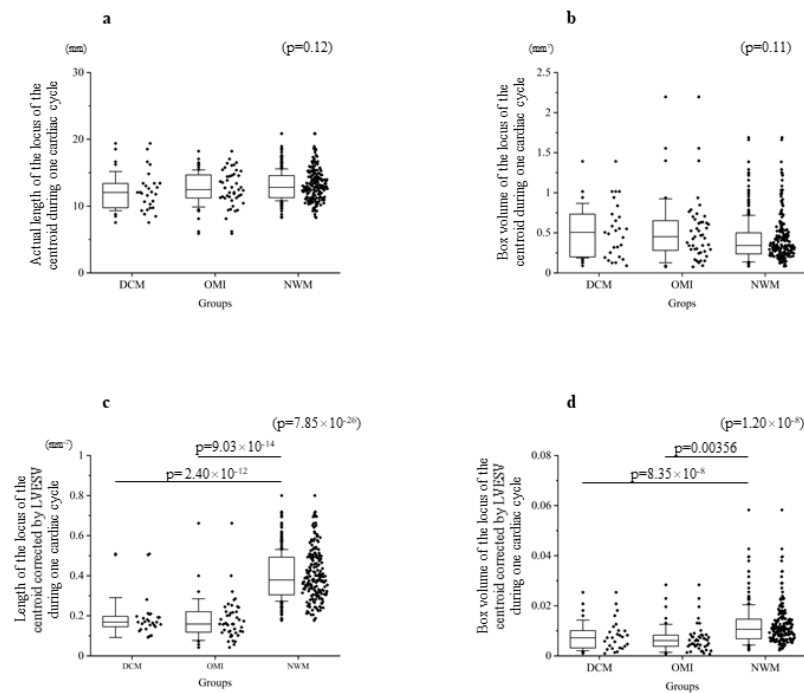
Fig. 2

Figure 2: The length and moving space of the locus of the centroid of the left ventricle for each group. The top panels show the actual length (a) and calculated box volume from the x-, y-, z-moving length (b). There was no significant difference among the groups. The bottom panels show the corrected data by LVESV. The corrected length of the locus of the centroid of the left ventricle (c) and the corrected volume (d) were significantly reduced in the DCM and OMI groups. DCM, dilated cardiomyopathy; LVESV, left ventricular end-systolic volume; NWM, normal wall motion; OMI, old myocardial infarction.

In the univariate analysis, the corrected data by LVESV of the LV centroid (concerning the distance, volume, and acceleration) together with the QRS duration, the value of NT-proBNP, and age were related to LVEF (Table 3). The corrected transfer distance for the longitudinal direction of the centroid by LVESV and the corrected total distance of the locus of centroid movement during one cardiac cycle by LVESV were excluded from the multivariate analysis because these data were considered variance inflation factors. Finally, a multivariate linear regression analysis revealed that an antero-posterior shift together with the transfer distance for the lateral direction of the LV centroid, NT-proBNP, and age

were strong predictors of the LVEF (multiple R^2: 0.5515; adjusted R^2: 0.5367; $p \leq 2.2 \times 10^{-16}$) (Table 4).

Factor	β	95% CI		SE	t-value	p-value
		Lower	Upper			
Transfer distance for the lateral direction of the centroid/LVESV	4,514.33	3,745.25	5,283.42	390.56	11.56	3.53×10^{-25}
Transfer distance for the A-P direction of the centroid/LVESV	1,135.67	963.35	1,308.00	87.51	12.98	5.55×10^{-30}
Transfer distance for the longitudinal direction of the centroid/LVESV	470.58	411.82	529.35	29.84	15.77	1.09×10^{-39}
Total distance of centroid movement during one cardiac cycle/LVESV	56.67	50.37	62.97	3.2	17.71	1.76×10^{-46}
Total moving box volume of the centroid/LVESV	632.81	461.37	804.25	87.06	7.27	4.32×10^{-12}
Maximum acceleration of the centroid during one cardiac cycle/LVESV	0.51	0.42	0.59	0.04	12.21	2.34×10^{-27}
Minimum acceleration of the centroid during one cardiac cycle/LVESV	−0.54	−0.63	−0.46	0.04	−12.23	1.89×10^{-27}
QRS duration	−0.22	−0.31	−0.13	0.04	−4.90	1.71×10^{-6}
NT-proBNP	−0.01	−0.01	0	0	−7.85	1.22×10^{-13}
Age	−0.11	−0.21	−0.02	0.05	−2.36	0.019

A-P, antero-posterior; CI, confidence interval; LVEF, left ventricular ejection fraction; LVESV, left ventricular end-systolic volume; NT-proBNP, N-terminal pro-brain natriuretic peptide; SE, standard error

Table 3: Univariate analysis for the prediction of LVEF

Factor	β	95% CI		SE	t-value	p-value
		Lower	Upper			
Intercept	51.86	43.66	60.06	4.16	12.46	7.20×10^{-28}
Transfer distance for the A-P direction of the centroid/LVESV	610.47	319.79	901.15	147.57	4.14	4.86×10^{-5}
Transfer distance for the lateral direction of the centroid/LVESV	1,880.96	667.94	3,093.98	615.82	3.05	0.00251
NT-proBNP	−0.00185	−0.00297	−0.00073	0.000568	−3.25	0.00131
Age	−0.11	−0.19	−0.03	0.04	−2.80	0.00546

A-P, antero-posterior, CI, confidence interval; LVEF; left ventricular ejection fraction, LVESV; left ventricular end-systolic volume, NT-proBNP; N-terminal pro-brain natriuretic peptide, SE, standard error

Table 4: Multivariate linear regression analysis for the prediction of the LVEF

In the analysis between markers of the LV centroid and diastolic function, the E/A ratio of the transmitral flow velocity was not correlated with any measurements of LV centroids. However, the E/e' correlated with the corrected transfer distance for the longitudinal direction of the centroid by LVESV ($r=-0.264$, $p=1.60\times10^{-5}$), the corrected box volume by LVESV ($r=-0.203$, $p=9.67\times10^{-4}$), and the corrected accelerations of the centroid by LVESV (maximum: $r=-0.171$, $p=5.67\times10^{-3}$, minimum: $r=0.157$, $p=0.011$). The left atrial volume was more strongly correlated with the corrected moving length of the LV centroid by LVESV for any direction (lateral: $r=-0.335$, $p=3.06\times10^{-8}$, antero-posterior: -0.303, $p=6.23\times10^{-7}$, longitudinal: -0.467, $p=1.85\times10^{-15}$), the corrected total distance of LV centroid movement by LVESV during one cardiac cycle ($r=-0.431$, $p=3.52\times10^{-13}$), and the corrected accelerations of the centroid by LVESV (maximum: $r=-0.515$, $p=4.97\times10^{-19}$, minimum: $r=0.475$,

$p=5.04\times10^{-16}$). Furthermore, the NT-proBNP was strongly correlated with any corrected transfer distance of the LV centroid for each direction (lateral: $r=-0.277$, $p=7.97\times10^{-6}$, antero-posterior: $r=-0.239$, $p=1.32\times10^{-4}$, longitudinal: -0.488, $p=1.77\times10^{-16}$), the corrected distance of total LV centroid movement by LVESV during one cardiac cycle ($r=-0.386$, $p=2.31\times10^{-10}$), the corrected box volume of the LV centroid ($r=-0.281$, $p=5.85\times10^{-6}$), and the corrected accelerations of the centroid (maximum: $r=-0.424$, $p=2.14\times10^{-12}$, minimum: $r=0.43$, $p=9.51\times10^{-13}$). Notably, the QRS width on electrocardiography showed weaker correlation with any transfer distance of the LV centroid for each direction (lateral: $r=-0.195$, $p=1.56\times10^{-3}$, antero-posterior: $r=-0.173$, $p=5.28\times10^{-3}$, longitudinal: -0.278, $p=5.55\times10^{-6}$) and corrected accelerations of the LV centroid by LVESV (maximum: $r=-0.282$, $p=3.73\times10^{-6}$, minimum: $r=0.276$, $p=6.36\times10^{-6}$).
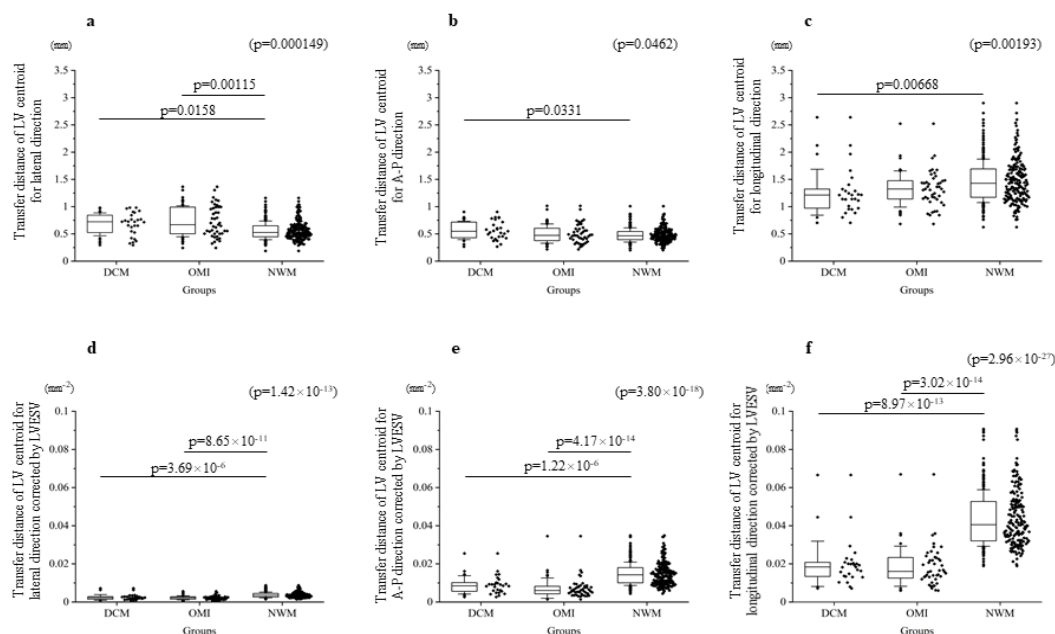
Fig. 3

Figure 3: Comparison of the transfer length of the locus of the centroid toward each direction. The top panels indicate the actual length for each direction: (a) lateral direction; (b) A-P direction; and (c) longitudinal direction. The bottom panels show the corrected length by LVESV. (d) shows the corrected length for the lateral direction by

LVESV. (e) shows the corrected length for the antero-posterior direction by LVESV. (f) indicates the corrected length for the longitudinal direction by LVESV. The corrected lengths of the locus of the centroid of the left ventricle by LVESV for each direction were clearly suppressed compared with those recorded in the NWM group. A-P, antero-posterior; DCM, dilated cardiomyopathy; LV, left ventricle; LVESV, left ventricular end-systolic volume; NWM, normal wall motion; OMI, old myocardial infarction.
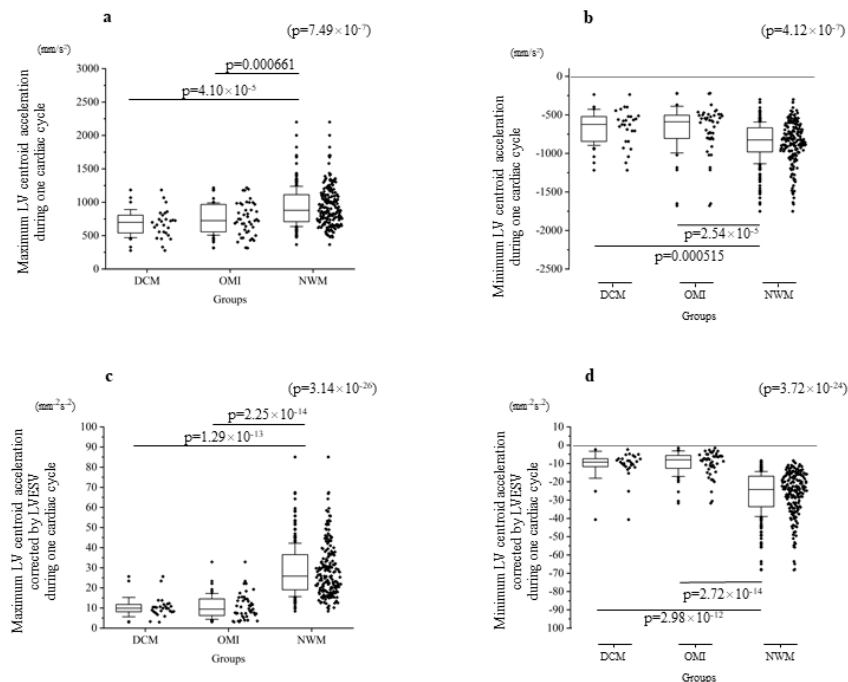
Fig. 4

Figure 4: Comparison of the maximal and minimum accelerations of the locus of the centroid of the left ventricle among the groups. The top panels indicate the real data ([a] for maximum acceleration, [b] for minimum acceleration), while the bottom panels show the corrected data by LVESV ([c] for the corrected maximal acceleration, [d] for the corrected minimum acceleration). When corrected by LVESV, the maximum and minimum accelerations in the abnormal wall motion groups were clearly reduced compared with those measured in the NWM group. DCM, dilated cardiomyopathy; LV, left ventricle; LVESV, left ventricular end-systolic volume; NWM, normal wall motion; OMI, old myocardial infarction.

5. Discussion

The present study compared several items derived from the locus of the LV centroid and the LVEF, which was a gold standard marker of LV systolic function. The objective of this investigation was to confirm that the locus of the LV centroid can predict LV systolic function. In addition, this study proposes a novel approach for the evaluation of abnormal LV wall motion. It was demonstrated that the LV centroid of the NWM group had moved like a mirror image of a β shape in a counterclockwise direction. In case of abnormal wall motion (e.g., dyssynchrony associated with DCM or LV aneurysm caused by an OMI), the corrected distance for any direction of the locus of the centroid by LVESV was significantly reduced compared with that noted for the NWM group, especially in the longitudinal direction. To increase the LVEF, it is suggested that the LV

centroid had to shift toward the anterior direction in an early phase of LV contraction. In patients with an extended LV chamber, the length which the LV centroid had moved during one cardiac cycle was limited to the enlarged cavity. This is because the cardiac muscle is confined in the cardiac sac, which is constructed by a tight fibrous membrane. To obtain sufficient stroke volume from the LV cavity, the LV centroid had to shift to the frontal position into the LV during the early contraction phase. This is because the blood stream had to be directed toward a LV outflow rather than a LV inflow positioned in a mitral ring. After moving toward the apical direction, it returned to the original position with two loose loops, which might have been caused by the cardiac translation of a diastolic phase and an atrial kick. The evaluation of LV wall motion (e.g., asynergy or dyssynchrony) using echocardiography is often subjective and depends on the experience of the physicians and expert technicians. It has been reported that strain is a good evaluator of the regional asynergy of ischemic heart disease [9-11]. In contrast, there are no standard markers available for the evaluation of mechanical dyssynchrony. In the case of ischemic heart disease, the reduced wall motion results from the ischemia of the dominated area associated with each coronary artery. Therefore, strain could detect the different ischemic area from cardiomyopathies which exhibited scattered fibrosis in the any part of the heart. Several studies [12-16] reported that echocardiographic markers detected using a tissue Doppler method, a M-mode technique, and the pulse Doppler technique were useful for the evaluation of mechanical dyssynchrony. However, the PROSPECT trial demonstrated that the aforementioned echocardiographic parameters failed to identify the responders to cardiac resynchronization therapy [4] because those evaluations were restricted to local or indirect information of the LV wall. The results of this study proposed the LV centroid as a novel approach, which requires information on each point of the LV

endocardium and each time point during a cardiac cycle. This method depends on the spatial and temporal information of the whole LV endocardium of the moving heart rather than selected information from a part of the LV and a limited time. Based on these facts, this novel approach may be useful for the selection of patients with mechanical dyssynchrony who could respond to cardiac resynchronization therapy. Patients exhibiting the following features may be responders to cardiac resynchronization therapy: 1) certified lesion viability in the area in which the LV wall motion was reduced; 2) simulation of a virtual LV wall motion after cardiac resynchronization therapy using a computing system, and 3) shift of the locus of the LV centroid toward an anterior direction in the early systolic phase using the virtual image. This is because LV good contraction does not always indicate an increase in LV systolic volume due to an increase in mitral regurgitation. In conclusion, the locus of the centroid of the LV associated with abnormal contraction of the heart did not resemble the mirror image of a β shape. Furthermore, the antero-posterior shift of the LV centroid was related to the LVEF. This novel approach may contribute to an objective evaluation of the LV mechanical dyssynchrony.

Limitations

In this study, the LV centroid calculated from two orthogonal views using a two-dimensional tracking method was utilized as a three-dimensional LV centroid. If a real-time three-dimensional speckle tracking system was available, the association with the LV centroid could have been examined in more detail.

Declarations

Conflict of Interest: None declared.

References

1. Mitchell C, Rahko PS, Blauwet LA, et al. Guidelines for Performing a Comprehensive Transthoracic Echocardiographic Examination in Adults: Recommendations from the American Society of Echocardiography. J Am Soc Echocardiogr 32 (2019): 1-64.

2. Ponikowski P, Voors AA, Anker SD, et al. ESC guidelines for the diagnosis and treatment of acute and chronic heart failure. Eur H J 37 (2016): 2129-2200.

3. Seferovic PM, Ponikowski P, Anker SD, et al. Clinical practice update on heart failure 2019: pharmacotherapy, procedures, devices and patient management. An expert consensus meeting report of the Heart Failure Association of the European Society of Cardiology. Eur H Fail (2019).

4. Chung ES, Leon AR, Tavazzi L, et al. Results of the predictors of response to CRT (PROSPECT) trial. Circulation 20 (2008): 8-16.

5. Ruschitzka F, Abraham WT, Singh JP, et al. EchoCRT Study Group, Cardiac-resynchronization therapy in heart failure with a narrow QRS complex. N Engl J Med 369 (2013): 1395-1405.

6. Baba H, Mori O, Miyaoka T, Development of 2D tissue tracking. MEDIX 43 (2005):19-22.

7. Miyoshi A, Nakamura Y, Kazatani Y, et al. The feasibility of substituting left atrial wall strain for flow velocity of left atrial appendage. Acta Cardiol 73 (2018): 125-130.

8. Kanda Y. Investigation of the freely available easy-to-use software 'EZR' medical statistics. Bone Marrow Transplant 48 (2013): 452-458.

9. Kusunose K, Yamada H, Nishio S, et. al. Validation of longitudinal peak systolic strain by speckle tracking echocardiography with visual assessment and myocardial perfusion SPECT in patients with regional asynergy. Circ J 75 (2011): 141-147.

10. Anwar A, Nosir Y, Alasnag M, et al. Quantification of left ventricular longitudinal strain by two-dimensional speckle tracking: A comparison between expert and non-expert readers. Int J Cardiovasc Imaging 29 (2013): 1451-1458.

11. Stankovic I, Putnikovic B, Cvjetan R, et al. Visual assessment vs. strain imaging for the detection of critical stenosis of the left anterior descending coronary artery in patients without a history of myocardial infarction. Eur Heart J Cardiovasc Imaging 16 (2015): 402-409.

12. Yu CM, Fung WH, Lin H, et al. Predictors of left ventricular reverse remodeling after cardiac resynchronization therapy for heart failure secondary to idiopathic dilated or ischemic cardiomyopathy. Am J Cardiol 91 (2003): 684-688.

13. Bax JJ, Bleeker GB, Marwick TH, et al. Left ventricular dyssynchrony predicts response and prognosis after cardiac resynchronization therapy. J Am Coll Cardiol 44 (2004): 1834-1840.

14. Yu CM, Chan YS, Zhang Q, et al. Benefits of cardiac resynchronization therapy for heart failure patients with narrow QRS complexes and coexisting systolic asynchrony by echocardiography. J Am Coll Cardiol 48 (2006): 2251-2257.

15. Pitzalis MV, Iacoviello M, Romito R, et al. Cardiac resynchronization therapy tailored by echocardiographic evaluation of

ventricular asynchrony. J Am Coll Cardiol. 40 (2002): 1615-1622.

16. Cazeau S, P Bordachar, G Jauvert, et al. Echocardiographic modeling of cardiac dyssynchrony before and during multisite stimulation: a prospective study. Pacing Clin Electrophysiol 9 (2003): 137-143.